JJEES

JJEES (2025) 16 (4): 407-417
ISSN 1995-6681

Jordan Journal of Earth and Environmental Sciences

Petro graphic and geochemical characterization of volcanic rock in Debre Tabor area, Northwestern Ethiopia: Implication for petrogenesis of felsic volcanic rock

Yaregal Bayih* and Amare Getaneh

Department of Geology, Debre Markos University, P.O. Box. 269, Debre Markos, Ethiopia

Received on April 10, 2025, Accepted on June 5, 2025

Abstract

Debre Tabor area, located on the Northwestern Ethiopian plateau and composed of Cenozoic volcanic rocks with minor intertrappean sediments. To understand the petrogenesis of these rocks, we conducted field investigations, petrographic studies, and geochemical analyses. The main volcanic products include basalt, trachyte, Ignimbrite, rhyolite, phonolite, and pyroclastic fall and flow deposit. Basalt rocks in the study area occur as a flat-lying topography, and under petrographic microscope view, they exhibit porphyritic and trachytic textures with phenocrysts of olivine, pyroxene, Fe-Ti Oxides, and P gioclase. Rhyolite rocks found by forming huge domes and show porphyritic and glomeroporphyritic texture with phenocrysts of sanidine, biotite and plagioclase minerals. The phonolite rock unit exhibit phenocryst of alkali feldspar, feldesphathoids (nepheline) and neason. The trachyte rock unit is formed by a volcanic plug. Debre Tabor volcanic rocks were formed from evolved magma as compared to a primary magma (with Ni: 400–500 ppm, Cr: > 1000 ppm and MgO: 10–15 wt.%, Hess, 1992). In chondrite and primitive mantle normalized REE patterns, both basaltic and felsic rocks exhibit enrichment of LREE (with a (La/Yb)N ratio ranging from 12.37 to 16.11), likely due to crustal contamination and an enriched mantle source of magma. In this pattern basaltic rocks show depleted trend of HREE, due to garnet or deep mantle source of magma. But felsic rocks show flat trend of HREE due to mafic crustal rock contamination effect. From the ratio of Ce/Pb versus MgO and Ce/Pb versus Nb/U, data points for Debre Tabor volcanic rocks fall outside of the mantle value (Ce/Pb; 25 ± 5; Nb/U = 47 ± 10) and plotted in the field of crustal/ lithospheric values, which give a strong indication for the crustal contamination effect of mantle-derived magma. All mafic rock samples in the study area have low Rb/Nb (0.5-0.97) and La/Nb (0.72-0.97) ratios and chondrite, primitive mantle normalized incompatible trace element patterns for basaltic rock that overlap with OIB, which confirms that the source of magma in the study area is from deep mantle with lower degree of partial melting. The geochemical analysis (positive correlation of Hf vs. La) shows that the basaltic rocks in the study area are co-genetic with felsic rocks and evolved through fractional crystallization and crustal contamination effects.

Keywords: *Crustal contamination; Crystal fractionation; Geochemistry and Petrogenesis, Magma evolution*

1. Introduction

The Ethiopian volcanic series can be divided into two main categories, based on their general lithological grouping: (I) Continental Flood Basalt (CFB), which is often covered by shield basalts and spans large swaths of the Balad's highland northwest and southeast plateaus in the Ter-tiary period, and (II) Rift volcanism, which is still actively occurring. One of the world's largest continental flood basalts (CFBs) is the Ethiopian CFB, which is among the youngest, least de-formed, and best-preserved uppermost volcanic rocks (Kieffer et al., 2004). One of the best instances of plume-related magmatism in an area of active extension is the volcanic province (Stewart et al., 1996, and references therein). It is a typical model to investigate how continen-tal crustal materials, sub-continental lithospheric mantle, and mantle plume contributed to the formation of plateau basalts (e.g. Courtillot et al., 1999). The Continental Flood Basalts (CFB) and the ensuing shield basalts have been the subject of studies on the Ethiopian plateau (e.g., Hofmann et al., 1997; Yirgu, 1997; Pik et al., 1998, 1999; Kieffer et al., 2004; Beccaluva et al., 2009; Corti, 2009; Natalie et al., 2017). According to Hofmann et al. (1997), the majority of the Ethiopian flood basalts formed a vast volcanic plateau 30 million years ago. Volcan-ism was mostly restricted along rifting regions following this formation, and several sizable shield volcanoes formed on the volcanic plateau's surface (Mohr & Zanettin, 1988).

Along the Ethiopian and Afar rifts, volcanic activity is still occurring today (Chazot & Bertrand, 2003). An area of over 600 000 km2 is covered by the Ethiopian flood basalts, also known as the trapseries, which are composed of a layer of basaltic and felsic volcanic rocks. In certain places, the layer is as thick as 2 km (Pik et al., 1999).

Transitional to tholeiitic, basaltic lava flows make up the majority of the Northern Ethiopian plateau, which is situated along the western flanks of the Afar Depression and the main Ethiopian Rift (MER) (Fig. 1a) (Mohr and Zanettin, 1988). Basalt makes up the majority of the volcanic rocks that cover the vast Ethiopian and Somalian plateau, which are part of the trap series (Abbate and Sagri, 1980). According to

* Corresponding author e-mail: yaregalbayih081@gmail.com

Hofmann et al. (1997), the continental flood basalts (CFB) found on the Ethiopian Plateaus in the south and north are among the youngest, least deformed volcanic rocks developed during the Oligocene time. Paleosoils are found at the base of the plateau's dominant basaltic lava flows (Pik et al., 1998). Plagioclase, clinopyroxene, and occasionally olivine phenocrysts characterize the mineralogical composition of the flood basalts, which often exhibit aphyric to sparsely phyric textures (Kieffer et al., 2004).

In Northern Ethiopia, the flood basalts are composed of high-Ti theoliites (HT1, HT2) in the southeast and generally low-Ti (LT) in the northwest (Pik et al., 1998). The Eastern section features the first high-Ti lava (HT1), while the Lalibela area, which is nearer the Afar depression, exposes the second high-Ti (HT2) series. Higher amounts of incompatible elements and extensive fractionation of REE are present in both the HT2 and HT1. In comparison to the HT1 basalts, the HT2 basalts are more magnesian and contain olivine and clinopyroxene phenocrysts. Although the flood basalt episode is dominated by basalts, it also includes substantial amounts of felsic lava flows and pyroclastic materials in the upper portions of the series, either interbedded in or covering the flood basalt (Ayalew and Yirgu, 2003). The Lima Limo rhyolites are interbedded with the low-Ti flood basalts in the Northwestern section of the plateau. In contrast, the Wegel Tena rhyolites are outcropped over the high-Ti basalts close to the Eastern Afar border. The plateau ignimbrites have a similar phenocryst assemblage of orthoclase, quartz, sanidine, and clinopyroxene, and their textures range from porphyritic to glassy (Ayalew & Yirgu, 2003).

The geochemistry of trace elements indicate that the majority of melts beneath the rift originate from the mantle, possibly from depths of 40–80 km, which correlates with the change from spinel to garnet peridotite (Latin et al., 1993). According to Peccerillo et al. (2003), the MER's mafic rocks have a porphyritic texture with phenocrysts of olivine, clinopyroxene, and Plagioclase. These rocks include hydrovolcanic lapilli, strombolian scoria, and lavas. On the other hand, felsic volcanic products dominate the Northern MER. According to Peccerillo et al. (2007), zoned magma chambers are responsible for the predominance of acidic volcanic products over mafic ones. Rhyolitic melt builds up at the top of these chambers, while mafic melts erupt when fractures reach the chamber's deeper layers. Silicic centers and a younger phase of basaltic volcanism are characteristics of Quaternary magmatism in the MER. While the silicic rocks are peralkaline, the basaltic lavas are slightly alkaline (Trua et al., 1999; Peccerillo et al., 2003). The plume, asthenosphere, and lithosphere are hypothesized to contribute to the partial melting of the mantle that produces mafic magmas (Gibson et al., 2006).

The majority of earlier research conducted on the volcanic plateau in Northern Ethiopia was limited to regional scale (e.g., Ayalew and Yirgu, 2003, Desta et al., 2014; Natali et al., 2016; Pik et al., 1998, 1999) and lacked a comprehensive study on the felsic volcanic rocks. In this study, petrographic and geochemical ' 'data's investigated to get information about the origin of felsic rocks and magma evolution processes.

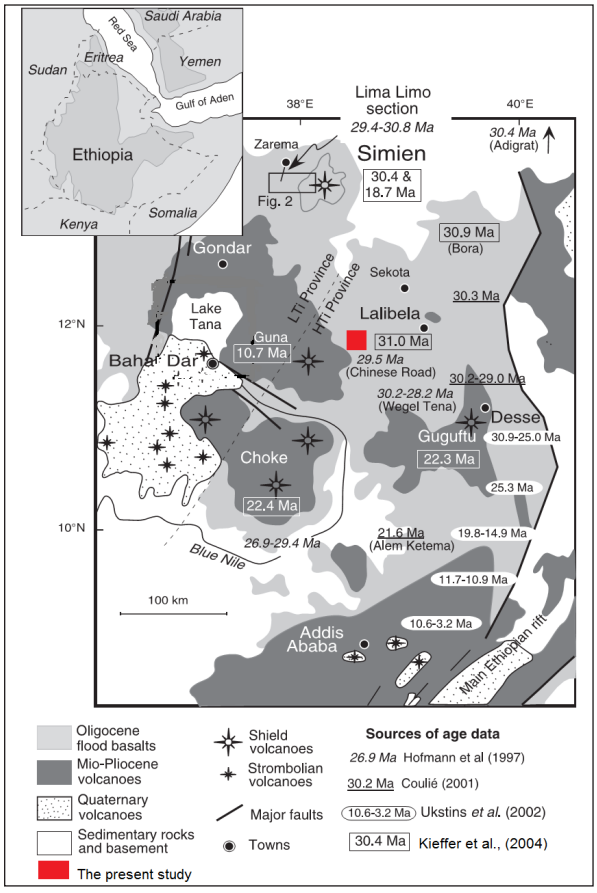

Figure 1. Map of the Northern part of the Ethiopian plateau showing the extent of the flood volcanism and the location and ages of the major shield volcanoes after Hofmann et al. (1997), Kieffer et al. (2004), and Ukstins et al. (2002). The dashed line shows the boundary between the LT and HT provinces as defined by Pik et al. (1999).

2. Sampling and Analytical Techniques

Sampling

In order to cover the complete volcanic succession, geological surveys and sampling were carried out using road and river cuttings that clearly display the volcanic rocks. Several lithological units were systematically mapped and described for various analytical investigations. The representative rock samples were taken from phonolite, rhyolite, trachyte, and basalt rocks, taking into account differences in texture, color, and weathering severity. Forty-five rock samples, each weighing between 0.75 and 1 kg, were gathered, labeled, and put in a plastic bag for various laboratory examinations.

Sample analysis

Nineteen representative rock samples - eight basalts, four rhyolites, four phonolites, and three trachytes were chosen, and each sample was split in half: one half was used for major and trace element chemistry, while the other half was used for thin section preparation. Thin sections were made in the Geological Survey of Ethiopia's (GSE) laboratory. The preparation process involves removing worn portions of the rock surface and using a diamond blade to cut each sample to the appropriate size.

Using a transmitted light microscope at Bahir Dar University's School of Earth Sciences, a thorough thin section description was completed, including rock name, mineral

identification, modal proportion, and textural descriptions. Geochemical investigations of bulk rocks were conducted at the Australia Laboratory Service (ALS) in Ireland. In a steel jaw crusher, materials were first cleaned, dried, and crushed into coarse chips that passed through a 70% 6 mm or fine rock chips that passed through 85% of a 2 mm. The samples were broken down using lithium metaborate, and the major and trace element contents were ascertained using a combination of Inductively Coupled Plasma-Mass Spectrometry (ICP-MS) and Inductively Coupled Plasma Atomic Emission Spectrometry (ICP-AES). Furthermore, a thermal decomposition furnace was used to calculate the loss on ignition (LOI) for each sample (1.0g) heated to 800°C for one hour. At last, all of the evaluated data were arranged and interpreted using several computer programs, including Microsoft Excel, ArcGIS, and GCDkit 4.1.

3. Results and Discussion

3.1 Results

3.1.1 Geology

Various volcanic rocks and their weathering derivatives comprise the majority of the research region (Figure 3b). These include unwelded tuff, phonolite, ignimbrite, trachyte, rhyolite, and basalt. In the area around Debre Tabor Town, basaltic rock was abundantly exposed and covered a flat terrain. It is black to dark grey, fine-grained, and aphyric to porphyritic. The phenocryst contains plagioclase, olivine, and pyroxenes. In the northwest of Debre Tabor town, a plug volcanic feature has exposed trachyte (figure B). On the outside of the plug, it is light gray and has an aphanitic texture; nevertheless, in the middle of the plug, phenocrysts of plagioclase and alkali feldspars were seen to have a coarse-grained structure. The loosely to more compacted form of tuff is its defining feature. Ignimbrite is found on top of tuffaceous rock, which has a range of clast sizes. Greenish to grey in color, the phonolite unit has a greasy sheen. Alkali feldspar and feldspatoids (nepheline) phenocrysts are present in this poorly to strongly porphyritic material. Several rhyolitic domes (figure A) were created when viscous magma rose effusively onto the surface and subsequently accumulated around the vent.

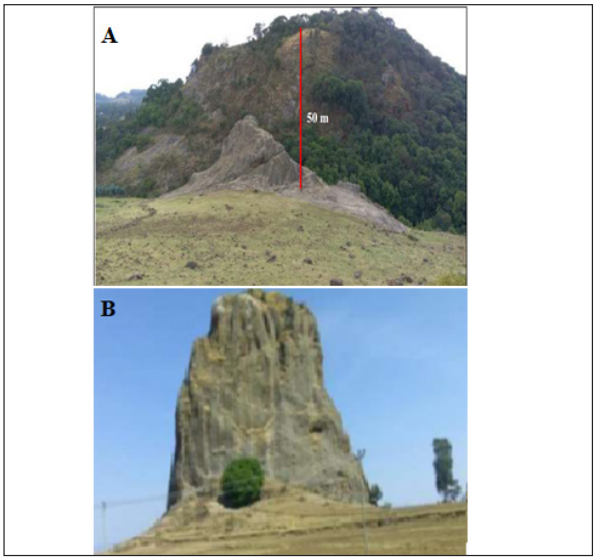

Figure 2. A and **B**: Rhyolitic dome and trachyte plug at Magere Mariam church and Amora Gedel, respectively.

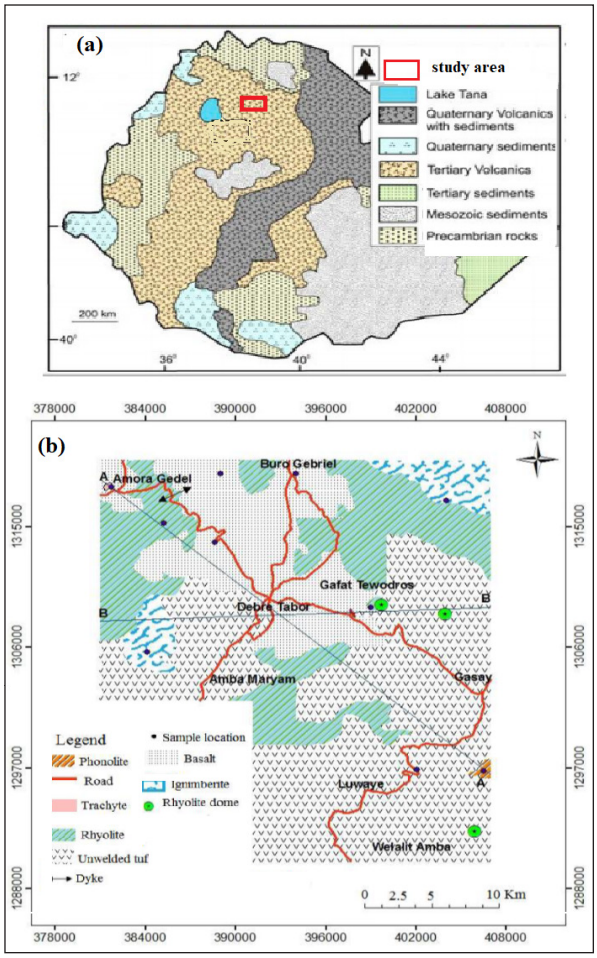

Figure 3. (**a**) Geological map of Ethiopia (modified after Merla et al. 1973), (**b**) simplified geological map of the study area

3.1.2 Petrography

The porphyritic texture of basaltic rock can be seen under a petrographic microscope to display euhedral to subhedral phenocrysts of pyroxene, olivine, and plagioclase (Figure 4A & B). The phenocryst assemblage is composed of 2-4 Vol.% pyroxene (augite), 5-7 Vol.% euhedral plagioclase lath, and approximately 3–4% olivine. Furthermore, the ground mass is composed of opaque, lath-shaped plagioclase, pyroxene (augite), and volcanic glass material. Rhyolite has 84 vol.% ground mass with a porphyritic structure and 16 vol.% phenocyst. The crystals are plagioclase, quartz, and subhedral alkali-feldspar. 6 Vol.% sanidine, 4-6 Vol.% plagioclase, 1-2 Vol.% opaque, and 1 Vol.% biotite are the phenocrysts. Quartz, plagioclase, and sanidine make up the groundmass. Trachyte is composed of 86 vol.% groundmass and 14 vol.% phenocrysts (figure 5 C & D). The phenocryst phases consist of <1 Vol.% Na-rich pyroxene, 2-3 Vol.% plagioclase, and 10-12 Vol.% massive euhedral to subhedral crystals of alkali feldspar (sanidine). Alkali feldspar (sanidine), Na-rich pyroxene, opaque, hornblende, biotite, and small amounts of volcanic glass are also found in the groundmass. Phonolite makes up 85 vol.% of ground mass and 13–20% of the phenocryst. 5-8 Vol.% lath-shaped alkali feldspar (sanidine), 7-9 Vol.% nepheline, 1-2 Vol.% sodic (Na-rich) pyroxene, and 2-3 Vol.% nosean make up the euhedral to subhedral phenocrysts. The groundmass consisted of nepheline, sanidine, opaque minerals, and pyroxene, high in sodium.

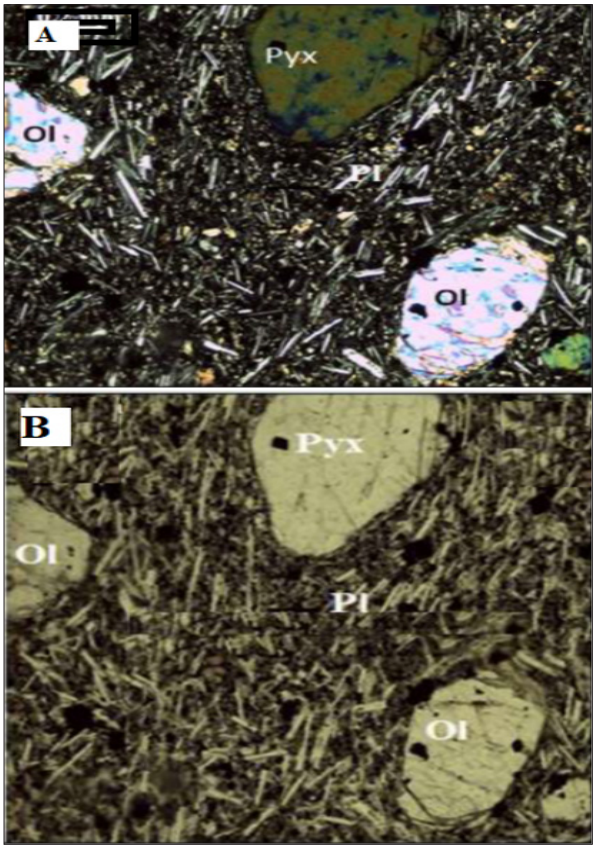

Figure 4. A & B. PPL and XPL view of Oligocene basalt with phenocrysts and microphenocrysts of olivine, pyroxene and plagioclase with inclusion of Fe-Ti Oxide in olivine minerals.

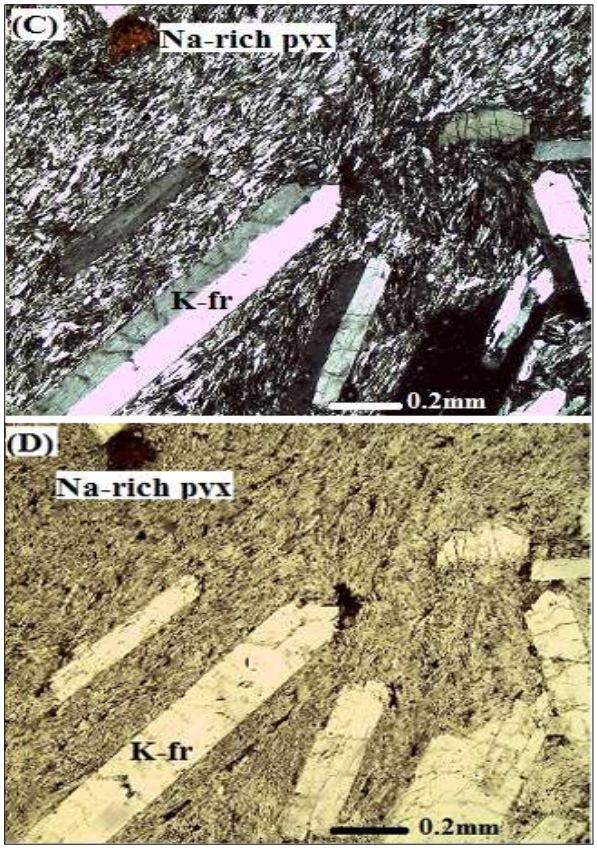

Figure 5. C & D. PPL and XPL view of trachyte unit having phenocrysts of biotite, k-feldspar, and Na-rich pyroxene with trachytic texture.

3.1.3 Geochemical results

The geochemical results in Table 1 show that all volcanic rock samples in the study area are characterized by low Ni (0.35-178 ppm) and Cr (7.54-350 ppm) contents, as well as low MgO contents (0.03–9.5 wt.%). These values are very low compared to those of a primary magma (with Ni: 400–500 ppm, Cr: > 1000 ppm, and MgO: 10–15 wt. %, Hess, 1992). This confirms that all volcanic rocks in the study area are not primary magma, instead all are fractionated.

Table 1. Major (wt. %) element ' 'data's of volcanic rock in the Debre Tabor area

Samples	SiO_2	Al_2O_3	Fe_2O_3	FeOt	CaO	MgO	Na_2O	K_2O	TiO_2	MnO	P_2O_5	SrO
DT1	43.3	16.4	12.85	11.565	9.86	5.47	3.37	1.72	3.43	0.21	1.25	0.14
DT2	42.2	14.95	13.2	11.88	10.43	8.06	3.11	1.12	3.66	0.18	1.3	0.19
DT3	46.25	15.54	12.77	9.57	9.07	6.31	3.27	1.62	3.41	0.21	1.26	0.14
DT4	43.8	15.01	12.25	10.05	9.16	9.5	3.85	1.61	2.65	0.17	0.93	0.12
DT5	47.1	16.5	12.63	7.55	8.54	5.36	4.01	1.74	3.32	0.201	1.23	0.13
DT6	43.2	15.1	13.4	11.56	8.54	7.76	4.55	1.54	2.42	0.21	1.09	0.1
DT7	44.1	15.02	12.01	10.02	9.07	6.41	3.77	1.72	3.4	0.41	1.46	0.24
DT8	45	14.22	11.03	9.85	9.76	5.47	3.47	1.42	3.53	0.31	1.35	0.24
DT9	58.1	23.4	3.41	2.93	0.87	0.29	8.62	6.01	0.39	0.31	0.03	0.02
DT10	59.5	21.73	4.32	2.03	0.45	0.17	9.06	6.45	0.32	0.31	0.13	0.02
DT11	62.1	19.2	2.21	1.97	0.22	0.03	6.72	5.8	0.42	0.01	0.67	0.01
DT12	57	19.76	3.21	1.98	1.02	0.25	7.03	6.58	0.57	0.09	0.27	0.03
DT13	55.3	20.34	3.78	3.57	1.54	0.5	8.53	5.03	0.54	0.06	0.34	0.02
DT14	68.3	15.05	2.43	2.187	0.33	0.15	6.56	5.17	0.42	0.11	0.06	0.01
DT15	56.4	22.2	3.52	3.168	0.91	0.4	8.17	5.84	0.43	0.3	0.02	0.01
DT16	61.8	19.55	2.32	2.088	0.29	0.06	6.12	5.72	0.51	0.01	0.66	0.01
DT17	71.1	14.91	1.64	1.476	0.6	0.3	5.59	5.19	0.6	0.02	0.11	0.02
DT18	67.5	16	2.45	2.23	0.43	0.25	6.45	5.05	0.45	0.11	0.05	0.01
DT19	66.1	16.97	2.46	2.35	0.41	0.15	5.43	4.12	0.39	0.12	0.03	0.01

Table 2. Trace element ' 'data's of Debre Tabor volcanic rock

Sample	Sc	V	Cr	Co	Ni	Cu	Zn	Cs	Rb	Ba	Sr	Th
DT1	19	295	30	33	11	26	116	0.29	43.4	695	1225	2.95
DT2	21	273	210	44	115	39	101	0.27	23.9	695	1615	2.65
DT3	19.2	298	33	33.6	11.02	25.2	115	0.29	43.21	687	1226	2.94
DT4	22	228	310	47	178	50	96	0.39	32.3	551	1060	4.92
DT5	18.37	271	29.7	32.82	11.3	26	118	0.28	44.1	691	1223	2.95
DT6	18.77	289	54.7	35.82	12.3	37	117	0.47	45.01	581	1013	3.45
DT7	17.02	268	53	36.6	10.02	35.2	99	0.28	39.21	677	1226	2.91
DT8	17	275	34	35.3	11.5	86	115	0.39	45.4	690	1235	2.85
DT9	1.3	14.23	9.4	1.5	1.2	1	192	1.33	199.5	17	21.3	33.4
DT10	1.2	12.23	7.54	0.45	0.35	1	189	1.04	199.8	19	21	34.4
DT11	1	25	9.7	0.9	2	2	75	0.23	128	116	87	17.3
DT12	1.13	26.3	9.82	1.03	2.01	2	72	0.21	124	113	89	16.5
DT13	1.04	16	11.02	1.09	1.2	1	193	1.34	193	14.9	23	31.3
DT14	4	9	10	1	1	1	81	0.43	109.5	366	51.2	15.8
DT15	1	15	10	1	1	1	194	1.35	199	15.6	22.3	32.3
DT16	1	26	10	1	2	2	80	0.26	126.5	115	89	16.15
DT17	2	8	30	1	1	1	36	0.61	94.4	367	173.5	11.4
DT18	3	9.83	10	1.3	1	1.2	78	0.4	98.7	364	51	13
DT19	3.2	9.87	10	1.4	1	1.2	77	0.3	83.45	302	43.3	12

Table 3. Trace element ' 'data's of Debre Tabor volcanic rock

Sample	La	Ce	Pr	Nd	Sm	Eu	Gd	Tb	Dy	Ho	Er	Yb	Lu
DT1	46.2	95.5	11.5	50.7	9.97	3.56	9.33	1.19	6.57	1.19	3.39	2.49	0.39
DT2	36.1	75.4	9.52	44.3	9.54	3.22	7.89	1.1	5.5	1.02	2.61	1.92	0.26
DT3	45.7	95.2	11.03	49.9	9.97	3.2	9.22	1.17	5.54	1.05	3.43	2.53	0.43
DT4	45.9	86.7	9.71	40.3	7.66	2.73	6.65	0.93	5.33	0.94	2.38	1.9	0.32
DT5	47.1	95.7	11.3	50.3	9.96	3.21	9.34	1.19	6.58	1.01	2.73	1.93	0.25
DT6	47.1	95.7	11.3	50.3	9.96	3.21	9.34	1.19	6.58	1.01	2.73	1.93	0.25
DT7	45.7	95.2	11.03	49.9	9.97	3.2	9.22	1.17	5.54	1.05	3.43	2.53	0.43
DT8	46.2	95.5	11.5	50.7	9.97	3.56	9.33	1.19	6.57	1.19	3.39	2.49	0.39
DT9	98.7	174	23.1	60.01	6.58	1.05	5.85	1.02	7.21	1.43	4.78	5.67	0.83
DT10	102	194	23.1	59	6.57	1.03	5.87	1.03	8.54	1.32	4.01	5.07	0.76
DT11	98.3	164	16.4	54.1	7.85	1.32	5.6	0.98	5.77	1.32	3.44	3.97	0.65
DT12	94.1	163	15.4	52.4	6.85	1.54	5.06	0.91	4.99	1.34	3.47	4.2	0.68
DT13	96.45	178	22.7	60.06	7.04	1.14	5.48	0.8	6.97	1.53	5.01	5.76	0.87
DT14	92.4	173	18.7	65.4	10.05	2.06	7.61	1.19	7.68	1.5	4.72	5.38	0.87
DT15	96.73	197	23.3	61.6	7.58	1.06	5.84	1	7.03	1.48	4.93	5.77	0.86
DT16	97.8	163	16.6	53.6	7.84	1.38	5.5	0.91	5.67	1.1	3.51	4.05	0.68
DT17	81.4	139	17.2	63.3	11.45	2.58	8.58	1.36	8.77	1.58	4.67	4.87	0.72
DT18	87	166	17.3	64	10.3	2.7	6.71	1.19	7.58	1.6	4.87	5.39	0.88
DT19	83.3	153	13.2	60.02	8.3	2.34	6.72	1.18	6.98	1.7	4.93	5.41	0.88

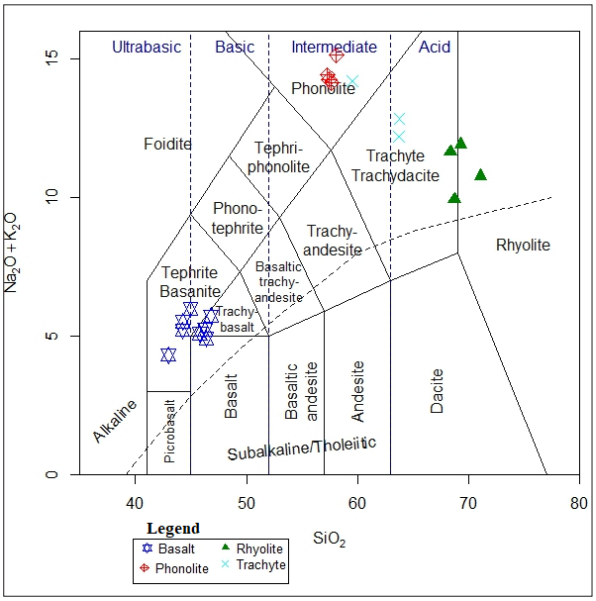

Figure 6. Total alkalis-silica (TAS) classification after Le Bas et al. 1986 for Debre Tabor volcanic rock.

All volcanic rock samples in the research area were plotted in the alkaline field using the total alkalis-silica (TAS) categorization following Le Bas et al. (1986) Figure 6.

In Debre Tabor volcanic rocks, the concentration of FeOt, CaO, TiO_2, and P_2O_5 declines as the weight percentage of SiO_2 increases from basalt to rhyolite (Figures 7 B, C, E, and F). Figure 7A and D show that while the SiO_2 concentration in weight percentage rises from basalt to phonolite, the concentration of Al_2O_3 and K_2O falls from phonolite to trachyte and from trachyte to trhyolite.

The mafic and felsic rocks of the study area (Figure 8 A and B) exhibit highly enriched lighter rare earth elements (LREE) and depletion of heavy rare earth elements (HREE) in basaltic rock samples, according to the chondrite and primitive mantle normalized incompatible trace element patterns (Boynton, 1984;McDonough and Sun, 1995).

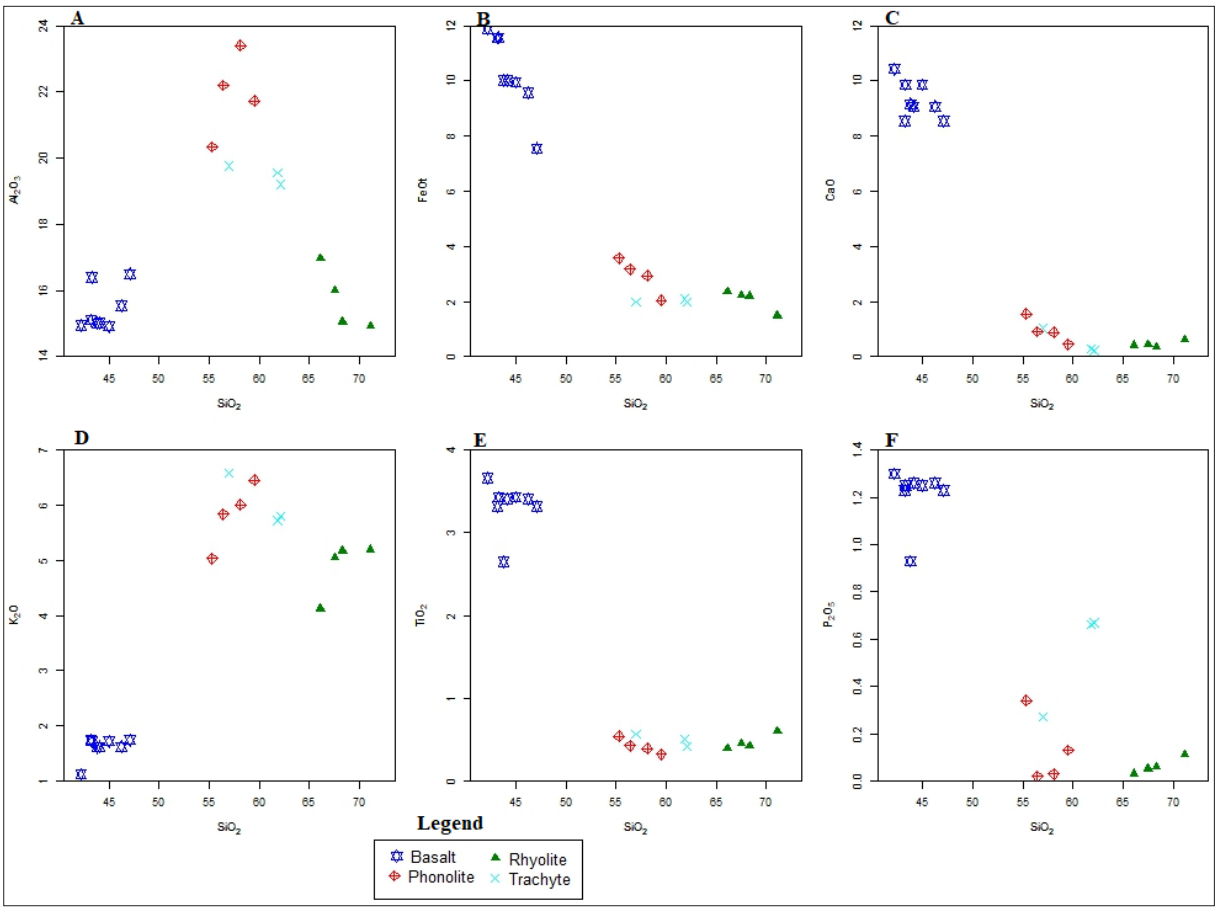

Figure 7. A – **F**. Variation diagrams of major elements versus SiO2 in wt% for Debre Tabor volcanic rocks

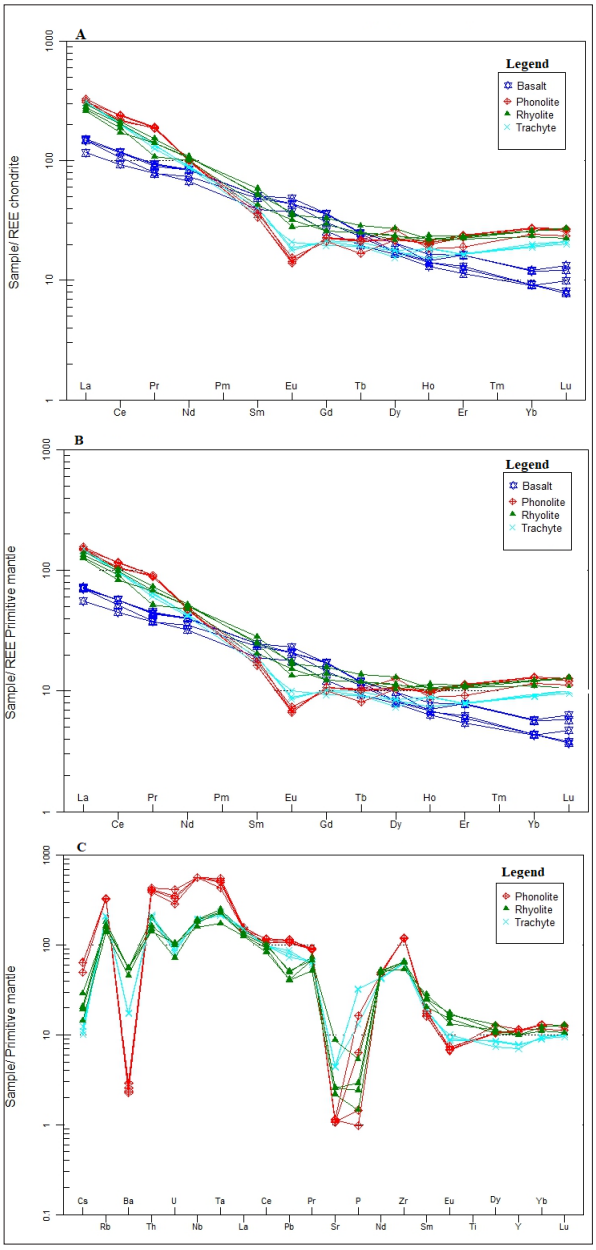

Figure 8. A, **B**, and **C**: Chondrite, primitive mantle REE, and primitive mantle normalized abundance pattern (Boynton, 1984, and Mc Donough and Sun 1995) for Debre Tabor volcanic rocks

4. Discussion

4.1. Fractional crystallization and crustal contamination

According to petrographic analysis, the main phenocryst phases for volcanic rocks in the study area are olivine, clinopyroxene, nepheline, opaque minerals, biotite, feldspars (including sanidine), and nosean. Figure 4 shows that olivine, clinopyroxene, plagioclase, and opaques are found as phenocryst phases in thin sections of basaltic rocks, but they are absent from felsic rocks, indicating that magma fractionation took place in the study area.

The geochemical results (Tables 1 & 2) indicate that the volcanic rocks in the study area have low concentrations of Ni (1 - 178 ppm), Cr (10 - 310 ppm), and MgO (0.03 - 9.5 wt.%), which is very low when compared to a primary magma (with Ni: 400–500 ppm, Cr: > 1000 ppm, and MgO: 10-15 wt. %, Hess, 1992). This result indicates that all the volcanic rocks in the study area are fractionated, and that the concentrations of MgO (wt.%), Ni, and Cr (ppm) decrease from basaltic rocks to felsic rocks as a result of olivine and clinopyroxene fractionation.

The concentration of FeOt, CaO, TiO_2, and P_2O_5 in weight percentage decreases with increasing SiO_2 concentration from basalt to rhyolite, according to variation diagrams of major elements versus SiO_2 in weight percentage (Figures 7 B, C, E, and F). This pattern indicates the fractionation (removal) of olivine or clinopyroxene, Ca-rich plagioclase, Fe-Ti Oxide, and apatite, respectively, in mafic rocks. The concentration of Al_2O_3 and K_2O in weight percentage increases from basalt to phonolite and then decreases from phonolite to trachyte and from trachyte to rhyolite (Figures 7 A & D) with increasing SiO_2 concentration. The data points for felsic, intermediate, and mafic rocks exhibit a positive correlation (the same orientation) (Figures 7 B, C, E, and F), confirming the co-genetic nature of these rocks. The fractional crystallization process was responsible for the evolution of magma from mafic to felsic.

The lighter rare earth elements (LREE) exhibit enrichment as a result of crustal contamination and magma derivation from enriched mantle sources in chondrite and primitive mantle normalized incompatible trace element patterns (Boynton, 1984 and Mc Donough and Sun, 1995) (Figures 8 A & B). In these patterns, the heavy rare earth elements (HREE) exhibit a depleted trend in basaltic rock samples due to garnet mineral fractionation, but a flat trend in felsic rock samples due to the mafic crustal rock contamination effect of magma. A negative anomaly in Eu suggests the fractionation of feldspar from the magma.

In felsic rock samples, the primitive mantle normalized incompatible trace element pattern (figure 8C) reveals a significant negative anomaly in the concentrations of P, Eu, Ba, and Sr. Fractional removal of apatite and garnet causes depletion in P and Eu, while fractionation of feldspar (sanidine and/or plagioclase) in mafic rocks causes depletion in Ba and Sr.

The Ce/Pb versus MgO weight percentage (Figure 9) and Ce/Pb versus Nb/U ratios (Figure 10) are beneficial because the OIB mantle value range is well established (Ce/Pb = 25 ± 5; Nb/U = 47 ± 10; Hofmann et al., 1986). The data points for the Debre Tabor basaltic rocks in figures 9 and 10 below are shown in the field of crustal/lithospheric values and fall outside of the mantle value (Ce/Pb; 25 ± 5; Nb/U = 47 ± 10). This provides clear evidence of the crustal contamination effect of mantle-derived magma.

Pearce (2008) states that volcanic rocks impacted by the crustal contamination effect will have data points above the MORB–OIB array in Nb/Yb versus Th/Yb plots, or that crustal input through contamination produces oblique trends to MORB–OIB that extend into the volcanic arc array. The existence of crustal contamination during the development of volcanic rocks in the research area is shown by data points of basaltic rocks that fall above the MORB–OIB array (Figure 11) below.

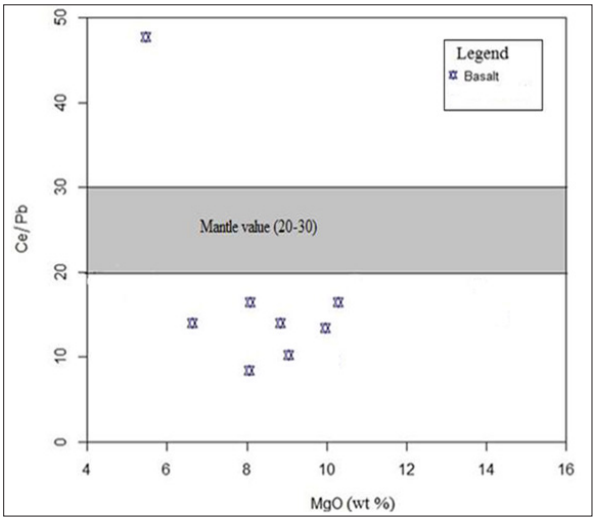

Figure 9. The ratio of Ce/Pb against MgO (wt.%) for Debre Tabor basaltic rocks. The shaded region indicates Ce/Pb ratio of the mantle value (25±5) after Hofmann et al. (1986)

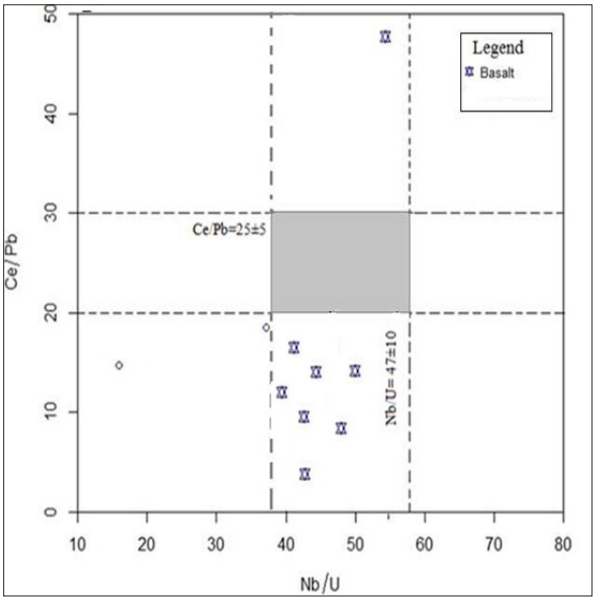

Figure 10. The ratio of Ce/Pb versus Nb/U for Debre Tabor basaltic rocks. The shaded region indicates the ratios of Ce/Pb (25±5) and Nb/U (47±10) for the mantle value after Hofmann et al. (1986)

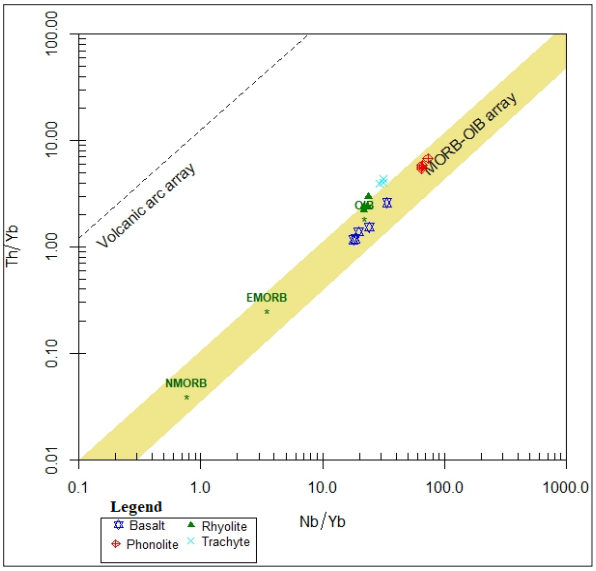

Figure 11. Nb/Yb versus Th/Yb diagram for the identification of crustal contamination (modified from Pearce 2008).

According to Dostal et al. (2017), the positive trends of incompatible trace elements (La vs. Hf) in both felsic and mafic rocks support the idea that both come from similar sources and effectively rule out melting of unrelated crustal rocks. Fessic volcanic rocks were formed from basaltic magma by a fractional crystallization process, according to the observed linear arrays of (Hf vs. La) (Figure 12) in the mafic and felsic rocks of the Debre Tabor volcanic rocks.

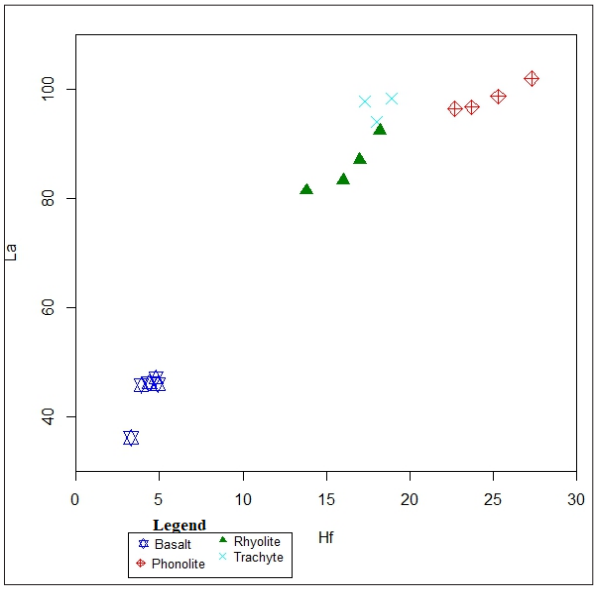

Figure 12. Variations of La vs. Hf (ppm) after (Dostal et al., 2017) for Debre Tabor volcanic rocks, showing the genetic relationship between the mafic and felsic rocks

4.2 Magma types

Hagos et al. (2010) state that the HT basalts have significantly greater TiO_2 levels (2.6–4.4 weight percent) than the LT basalts, which have the lowest TiO_2 values (1.99–2.56%). In the research area, the TiO_2 concentration of the basaltic rock sample ranges from 2.42 to 3.66, confirming that the volcanic rocks are classified as HT basalts. Ti/Y and Nb/Y ratios in high-Ti basalts range from over 450 to 0.4, respectively (Pik et al., 1998). Data points for the study area's basaltic rock fall within the high-Ti basalt (HT) field, as shown in Figure 13 below.

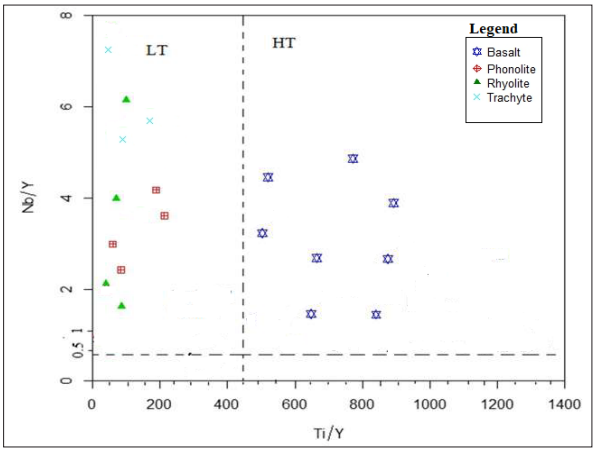

Figure 13. Nb/Y versus Ti/Y diagram of Debre Tabor volcanic rocks for the identification of low-Ti (LT) and high-Ti (HT) basalts (the figure is modified after Pik et al., 1998).

4.3 Degree of partial melting

Following the classification of total alkalis-silica (TAS) by Le Bas et al. (1986), all volcanic rock samples in the study area were plotted in the alkaline field (Figure 6). Figures 8A and B, which depict the pattern of chondrite and primitive mantle normalized rare earth elements (REEs) for basaltic rocks in the research area, demonstrate a reduction in heavy rare earth elements (HREEs). The alkaline field in the TAS diagram and the heavy rare earth element depletion patterns so indicate that the magma in the studied area originated from the deep mantle with a reduced degree of partial melting.

Pearce (2008) asserts that the Nb/Yb against TiO2/Yb plot can be used to determine the magma's origins. The point data for basaltic rocks in the research area (Figure 14A) fall within the OIB array's field, indicating that the deep mantle, which had a low degree of partial melting, was the source of the magma in the study area. To differentiate between garnet peridotite and spinel melting, the ratios of La/Sm and Sm/Yb are beneficial (Lassiter and DePaolo, 1997).

Consequently, the Debre Tabor volcanic rocks are plotted in the primitive mantle value (Figure 14B) and have high La/Sm (2.65–5.99) and Sm/Yb (2.52–4.97) ratios. In general, a smaller degree of partial melting of garnet peridotite produced the magma in the research location.

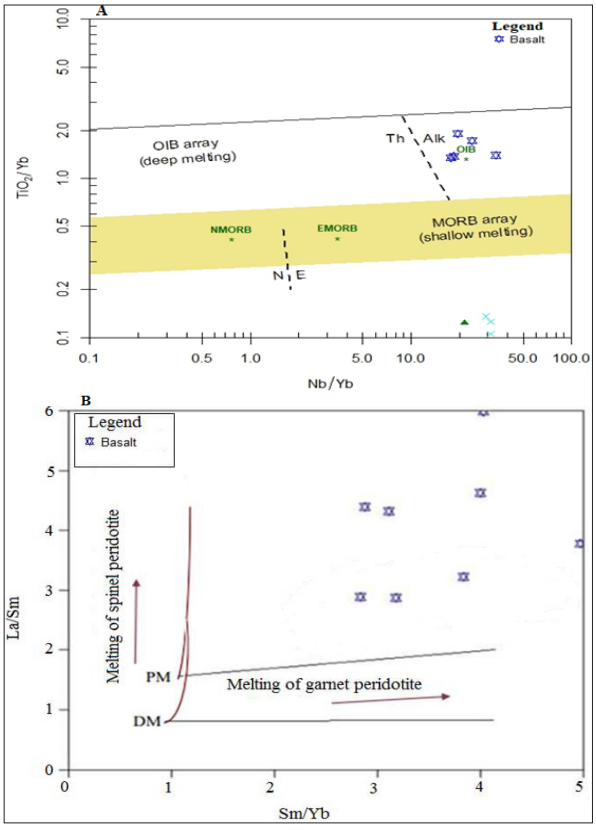

Figure 14. A & B. Nb/Yb versus TiO2/Yb diagram (Pearce, 2008) and Ratios of La/Sm versus Sm/Yb for Debre Tabor volcanic rocks with primitive mantle (PM) and depleted mantle (DM) compositions (Ayalew et al. 2006).

4.4 Comparison with N - MORB and OIB

4.4.1 Mantle source composition

Pyroxene and olivine were found as phenocrysts in basaltic rocks, as shown by petrographic views of thin sections (Figure 4). This phenocryst provided support for the mantle source of magma in the research area. The composition of volcanic rocks that are created by the fractional crystallization of magma from the mantle should continuously shift from mafic to intermediate to felsic rocks (Kessel et al., 1998). The research area's volcanic rocks exhibit a consistent compositional shift from mafic to intermediate to felsic, confirming the mantle as the source of the magma.

Very high LILE/HFSE ratios (such as Rb/Nb and La/Nb) are characteristic of magmacreated by the partial melting of crustal rock (Pearce et al., 1984). However, the ratio of this element in Debre Tabor volcanic rock is extremely low (0.72 – 0.97), confirming that the volcanic rocks in the research area originated from the mantle.

Figures 15A and B, which represent the chondrite and primitive mantle normalized incompatible trace element patterns for basaltic rocks in the study, demonstrate a depletion of heavier rare earth elements (HREE) in comparison to N-MORB and a high enrichment of lighter rare earth elements (e.g., the (La/Yb)N ratio ranges from 12.37 to 16.11) (after Sun and McDonough, 2016). The deep mantle is the source of magma in the research area, as confirmed by the normalized patterns (Figures 15A and B) for the basaltic rocks in the area overlaid on OIB (following Sun and McDonough, 2016). Because of the enriched mantle source, fractional crystallization, and crustal contamination effects on the magma, there is a high enrichment in lighter rare earth elements.

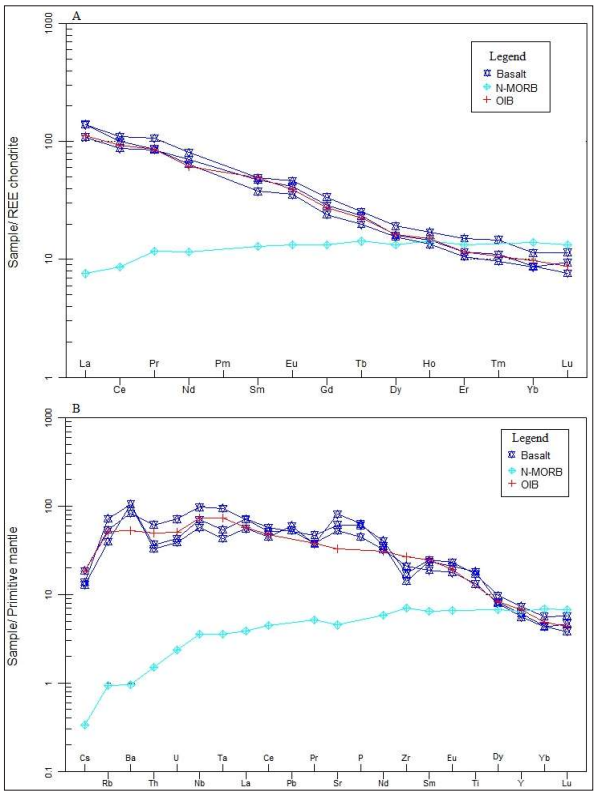

Figure 15. A & B. Chondrite and Primitive mantle normalized incompatible trace elements abundance pattern for Debre Tabor basaltic rocks after Nakamura (1974) and McDonough and Sun (1995), respectively. OIB and N-MORB data are used for comparison after Sun and McDonough (2016)

5. Conclusion and Recommendation

5.1. Conclusion

Based on field observations, petrography, and whole-rock geochemical studies (major and trace elements), the geology of the study area is mainly composed of basalt, ignimbrite, rhyolite, phonolite, trachyte flows, pyroclastic flow and fall deposits.

Debre Tabor volcanic rocks were not formed by solidification of primary magma; instead, it was formed from evolved magma, which was affected by crustal contamination and crystal fractionation evolutionary process. The LREE and highly incompatible trace element enrichment in felsic rocks is due to crystal fractionation, an enriched mantle source, and the effect of magma contamination on the crust.

The geochemical analysis (major and trace element analysis) shows that the mafic and felsic rock units in the Debre Tabor area have a co-genetic origin and formed by partial melting of deep mantle rock which is garnet peridotite with lower degree of partial melting. The Rb/Nb and La/Nb depleted character of the mafic lavas reflects the dominant contribution from the mantle plume during the genesis of volcanic rocks in the study area.

Basaltic rocks in the study area are grouped under high-Ti basalt, but the point data for felsic rocks fall under the low-Ti field.

5.2. Recommendations

For a better understanding of the properties of the magma source, age determinations, and geochemical processes involved in producing the rock suites of the Debre Tabor area, isotope geochemistry, mineral chemistry, and whole-rock studies should be conducted. Near Magere Mariam Church, there are also iron resources, and qualified businesses should be announced for exploration.

References

Ayalew, D., Yirgu, G., 2003. Crustal contribution to the genesis of Ethiopian plateau rhyolitic ignimbrites: basalt and rhyolite geochemical provinciality. J. Geol. Soc. 160 (1), 47–56.

Beccaluva et al. (2009). Continental flood basalts and mantle plumes: a case study of the northern Ethiopian Plateau. J. Petrology.37, 743–854.

Berhe, S.M., Desta, B., Nicoletti, M., Teferra, M., (1997). Geology, geochronology and geodynamic implications of the Cenozoic magmatic province in W and SE Ethiopia. J. Geol. Soc.London 144, 213–226.

Chazot G, Bertrand H (2003). Mantle sources and magma-continental crust interactions during early Red Sea-Aden rifting in Southern Yemen:. Journal of Geophysical Research 98:1819–1835.

Desta, M.T., Ayalew, D., Ishiwatari, A., Arai, S., Tamura, A., (2014). Ferropicrite from the Lalibela area in the Ethiopian large igneous province. J. Mineral. Petrol. Sci. 109 (4), 191–207.

Dostal, J., Hamilton, T.S., Shellnutt, J.G., (2017). Generation of felsic rocks of bimodal volcanic suites from thinned and rifted continental margins: geochemical and Nd, Sr, Pb-isotopic evidence from Haida Gwaii, British Columbia, Canada. Lithos 292, 146–160.

G. Corti. (2009). Continental rift evolution: from rift initiation to incipient break-up in the Main Ethiopian Rift, East Africa. Earth Sci. Rev.

Hagos M, Koeberl C, Kabeto K, Koller F (2010), Geochemical characteristics of the alkaline basalts and the phonolite-trachyte plugs of the Axum area, northern Ethiopia. Austrian J Earth Sci 103:153–170.

Hofmann, C., Courtillot, V., Feraud, G., Rochette, P., Yirgu, G., Ketefo, E. and Pik, R. (1997). Timing of the Ethiopian flood basalt event and implications for plume birth and global change . Nature .389, 338-341.

K. Stewart et al.(1996). Mantle plume and lithosphere contributions to basalts from southern Ethiopia. Earth Planet Sci. Lett.

Kessel, R., Stein, M. and Navon, O.,(1998). Petrogenesis of late Neoproterozoic dikes in the northern Arabian-Nubian Shield: implications for the Origin of A-type granites. Precambrian Research 92, 195–213.

Kieffer, B., Arndt, N., Lapierre, H., Bastien, F., Bosch, D., Pecher, A., Yirgu, G., Ayalew, D.,Weis, D., Jerram, D.A., Keller, F., Meugniot, C., (2004). Flood and shield basalts from Ethiopia: magmas from the African superswell. Journal of Petrology 45, 793–834.

Lassiter, J. C. and DePaolo, D. J. (1997). Plume/lithosphere interaction in the generation of continental and oceanic flood basalts: chemical and isotopic constraints. Large Igneous Provinces, Geophys. Monogr. 100, 335–355, American Geophysical Union, Washington, D.C.

Le Bas, M. J., Le Maitre, R. W., Streckeisen, A. and Zanettin, B. (1986). A chemical classification of volcanic rocks based on the total alkali-silica diagram. Journa of Petrology. 27, 745–750.

Natali, C., Beccaluva, L., Bianchini, G., Ellam, R.M., Savo, A., Siena, F., Stuart, F.M., 2017. High-MgO lavas associated to CFB as indicators of plume-related.

S.A. Gibson et al. (2006). The late Cretaceous impact of the Trinidade mantle plume: evidence from large volume mafic potassic magmatism in SE Beazil. J. Petro.

Sun and McDonough (2016). Chemical and isotopic systematics of oceanic basalt: implications for mantle composition and processes. Pennsylvania State University, 313-341.

Trua et al. (1999). Origin by fractional crystallization of transitional basalt for the Asela-Ziway pantellerites. Crustal control in the genesis of Plio-Quaternary bimodal magmatism of the Main Ethiopian Rift (MER) : Geochemical and isotopic (Sr, Nd, Pb) evidence. Chemical Geology 168(1):1-3

Merla G, Abbate E, Canuti P, Sagri M, Tacconi P. (1973). Geological map of Ethiopia and Somalia, scale 1:2,000,000. Consiglio Nazionale delle Ricerche, Roma.

Merla, G., Abbate, E., Azzaroli, A., Bruni, P., Fazzuoli, M., Sargi, M. and Tacconi, P. (1979). A geological map of Ethiopian and Somalia: Comment. Petgamon, 95p.

Mohr, P. and Zanettin, B. (1988). The Ethiopian flood basalt province. In: Macdougall, J. D. Continental Flood Basalts. Dordrecht:Kluwer Academic, pp. 63-110.

P.C. Hess. (1992). Phase equilibria constraints on the origin of ocean floor basalts

Pearce, J.A. and Cann, J.R. (2008). Tectonic setting of basic volcanic rocks determined using trace elements analyses. Earth and Planetary Science Letters, 19, 290-300.

Peccerillo, A., Barberi, M.R., Yirgu, G., Ayalew, D., Barbieri, M.W.U.T.W., Wu, T.W. (2003). Relationships between mafic and peralkaline silicic magmatism in continental rift settings: a petrological, geochemical and isotopic study of the Gedemsa volcano, central Ethiopian rift. J. Petrol. 44 (11), 2003–2032.

Pik, R., Deniel, C., Coulon, C., Yirgu, G., Hofmann, C., Ayalew, D., 1998. The northwestern Ethiopian Plateau flood basalts: classification and spatial distribution of magma types. J. Volcanol. Geoth. Res. 81 (1), 91–111.

Pik, R., Deniel, C., Coulon, C., Yirgu, G. and Marty, B. (1999).

Isotopic and trace element signatures of Ethiopian basalts: evidence for plume-lithospheric interactions. Geochimical Cosmochimica Acta 63,2263-2279.

Ukstins, I.A., Renne, P.R., Wolfenden, E., Baker, J., Ayalew, D., Menzies, M., 2002. Matching conjugate volcanic rifted margins: 40Ar/39Ar chrono-stratigraphy of preand syn-rift bimodal flood volcanism in Ethiopia and Yemen. Earth Planet Sci. Lett. 198 (3–4), 289- 30.

V. Courtillot et al. (1999). On causal links between flood basalts and continental breakup. Earth Planet Sci. Lett.